Cellular Physiology and Biochemistry

Cell Physiol Biochem 2018;45:2506-2515

DOI: 10.1159/000488269

Published online: March 19, 2018

Accepted: February 20, 2018

Original Paper

Dysregulated MiR-3150a-3p Promotes Lumbar Intervertebral Disc Degeneration by Targeting Aggrecan

Bin Zhang[a] Wei Guo[b] Chao Sun[a] Hui-Quan Duan[a] Bing-Bing Yu[a] Kun Mu[c] Yue-Yan Guan[d] Yan Li[a] Shen Liu[a] Yang Liu[a] De-Xiang Ban[a] Wen-Dong Ruan[a] Xiao-Hong Kong[e] Cong Xing[a] Guang-Zhi Ning[a] Shi-Qing Feng[a]

[a]Department of Orthopaedics, Tianjin Medical University General Hospital, Heping District, Tianjin, [b]Department of Orthopaedics, Hebei province Cangzhou Hospital of integrated traditional and Western Medicine (Cangzhou No.2 Hospital), Cangzhou, [c]Department of Breast Surgery, Hebei province Cangzhou Hospital of integrated traditional and Western Medicine (Cangzhou No.2 Hospital), Cangzhou, [d]Department of Endocrinology, Tianjin Third Central Hospital, Tianjin, [e]School of Medicine, Nankai University, Tianjin, P. R. China

Key Words
Intervertebral disc degeneration • MicroRNA • MiR-3150a-3p • Nucleus pulposus • Aggrecan

Abstract
Background/Aims: Low back pain has become one of the most common musculoskeletal diseases in the world. Studies have shown that intervertebral disc degeneration (IDD) is an important factor leading to low back pain, but the mechanisms underlying IDD remain largely unknown. Research over the past decade has suggested critical roles for microRNAs (miRNAs) in natural growth and disease progression. However, it remains poorly understood whether circular RNAs participate in IDD. ***Methods:*** Clinical IDD samples were collected from 20 patients who underwent discectomy. Weighted gene co-expression network analysis was used to identify the co-expression miRNA network modules (highly co-expressed clusters of miRNAs) that were associated with IDD grade. ***Results:*** miR-3150a-3p was the most significantly up-regulated miRNA in module "Blue." Notably, aggrecan (*ACAN*) was identified as a direct target gene of miR-3150a-3p and *ACAN* expression was regulated by miR-3150a-3p. Overexpression of miR-3150a-3p decreased *ACAN* expression in nucleus pulposus cells, whereas inhibition of miR-3150a-3p increased *ACAN* expression. In addition, *ACAN* expression was negatively correlated with IDD grade. ***Conclusion:*** Our study suggests that the reduction of *ACAN* expression induced by the upregulation of miR-3150a-3p might participate in the development of IDD.

B. Zhang, W. Guo and C. Sun contributed equally to this work.

Shi-Qing Feng

Department of Orthopaedics, Tianjin Medical University General Hospital, 154 Anshan Road, Heping District, Tianjin (China)
E-Mail sqfeng@tmu.edu.cn

Introduction

Intervertebral disc degeneration (IDD) is characterized by increased extracellular matrix breakdown and abnormal matrix synthesis, which contribute to reduced hydration, loss of disc height, and decreased ability to absorb load [1, 2]. It is considered as the predominant source of chronic low back pain and spine-related disease, which causes a major economic and social burden affecting millions of people worldwide [3]. It is estimated that as much as 84% of the population suffers from low back pain at some point in their life, whereas 10% are chronically disabled [4]. The main clinical manifestations of IDD are disc herniation, vertebral instability, and spinal stenosis. However, our ability to treat IDD effectively is hampered by an incomplete understanding of the physiological processes that control intervertebral disc development, function, and disease. Today, IDD is still treated with symptomatic interventions that do not provide adequately improved outcomes, as no disease-modifying drugs are available [5]. Consequently, the clinical management of IDD pathologies remains severely limited, with no options yet for early intervention or predictive patient screening. Therefore, understanding the pathophysiology and molecular mechanism underlying IDD appears to be imperative for its diagnosis and the development of novel therapeutic approaches. Numerous studies indicate that a variety of cellular events are disturbed in the progression of IDD, including matrix synthesis, nucleus pulposus (NP) cell apoptosis, and cytokine expression [6-11].

Increasing evidence has shown that IDD is a multifaceted spinal disease. Both genetic and environmental factors contribute to IDD, but genetic factors are considered to be the greatest contributors [12-15]. The genetic machinery ranges from single nucleotide variants and coding genes to newly defined noncoding RNAs (ncRNAs). Recent whole-genome sequencing studies have greatly expanded our understanding of the human genome [16, 17]. As a large set of transcript products of the human genome, ncRNAs account for 98% of the human genome devoid of protein-coding function. Overwhelming evidence indicates that ncRNAs, including microRNAs (miRNAs), exist widely in living organisms. Moreover, ncRNAs play critical roles in a variety of physiological processes pertaining to gene expression [18, 19]. Although a number of molecular drivers of IDD have been described over the years, miRNAs have emerged only very recently as key players in the pathogenesis of IDD [20-22]. Accumulating evidence indicates that miRNAs are frequently dysregulated in the development of IDD [23].

The aim of this study was to investigate the role of miR-3150a-3p in IDD by targeting aggrecan, and we hypothesized that dysregulated miR-3150a-3p may promote IDD. Weighted gene co-expression network analysis (WGCNA) was performed to identify several IDD grade-correlated miRNAs, and discovered that miR-3150a-3p expression was significantly upregulated in degenerative NP tissues versus control tissues and the expression level of miR-3150a-3p was significantly correlated with degeneration grade. Subsequently, we systematically validated the role of miR-3150a-3p in a series of experiments performed in cultured human NP cells.

Materials and Methods

Clinical specimens

This study was approved and supervised by the Ethics Committee of Tianjin Medical University General Hospital and Hebei Province Cangzhou Hospital of Integrated Traditional and Western Medicine. Written informed consent was obtained from patients for research purposes. Human lumbar degenerative NP specimens were obtained from 20 patients with IDD undergoing discectomy in the Tianjin Medical University General Hospital and Hebei Province Cangzhou Hospital of Integrated Traditional and Western Medicine. The control samples were taken from 20 age- and sex-matched patients with fresh traumatic lumbar fracture who underwent anterior decompressive surgery because of neurological deficits (Table 1). IDD grade was classified as described previously [24].

Microarray data

The miRNA expression data set (GSE63492) was downloaded from the Gene Expression Omnibus database (http://www.ncbi.nlm.nih.gov/geo) [15], which contained 5 human NP samples derived from patients with IDD and 5 derived from cadaveric disc as normal controls. The platform was a GPL19449 Exiqon miRCURY LNA microRNA Array for miRNA. Probe annotation files were also acquired.

Table 1. Clinical features of the study population. [a]Student's t-test. [b]Two-sided chi-squared test. BMI, body mass index

Variable	Normal (n = 20)	IDD (n = 20)	*P*
Age(years, mean, SD)	37.75 (8.47)	41.15 (11.19)	0.286[a]
BMI (Kg/m^2)	24.08 (1.82)	25.06 (2.15)	0.129[a]
Sex (%)			
Male	13 (65)	14 (70)	0.736[b]
Female	7 (35)	6 (30)	
Grade			
1	-	1 (5)	
2	-	2 (10)	
3	-	5 (25)	
4	-	6 (30)	
5	-	6 (30)	

Inferring degeneration grade-associated co-expression miRNA network modules

Before network inferring, raw data were converted into recognizable format with the affy package of R, and missing values were then imputed by a method based on k nearest neighbors [25], then the data were normalized with the median method [26]. The co-expression miRNA network modules (highly co-expressed clusters of miRNAs) were inferred from the IDD grade-associated miRNAs using WGCNA, an R package [27]. WGCNA network construction and module detection were conducted using an unsigned type of topological overlap matrix, a power β of 10, a minimal module size of 10, and a branch merge cut height of 0.25. The module eigengene (the first principal component of a given module) value was calculated and used to test the association of modules with IDD grade in the 10 samples. The most significant module of miRNAs was visualized using R.

Identification of key miRNAs in IDD

Differential analysis was performed using the limma package [28] between the degeneration samples and controls in module "Blue" (Table 2). The limma package involves pre-processing, exploratory data analysis, differential expression testing, and pathway analysis, with the results obtained informing future experiments and validation studies (http://www.bioconductor.org/packages/release/bioc/vignettes/limma/inst/doc/usersguide.pdf). The first was the design matrix, which indicated in effect which RNA samples were applied to each array. The second was the contrast matrix, which specified which comparisons you would like to make between the RNA samples. For statistical analysis and assessing differential expression, limma uses an empirical Bayes method to moderate the standard errors of the estimated log-fold changes. The basic statistic used for significance analysis is the moderated t-statistic, which was computed for each probe and each contrast. Moderated t-statistics lead to p-values in the same way that ordinary t-statistics do, except that the degrees of freedom are increased, reflecting the greater reliability associated with the smoothed standard errors. Limma provided the functions top Table and decided Tests, which summarize the results of the linear model, perform hypothesis tests, and adjust the p-values for multiple testing. The results include (log-) fold changes, standard errors, t-statistics, and p-values [29]. |Log(fold change)| > 1 and adj. p-value < 0.05 were set as the cut-offs to screen out differentially expressed miRNAs.

Isolation and culture of human NP cells

Tissues specimens were washed twice with phosphate-buffered saline, and the NP was separated from the annulus fibrosus using a stereotaxic microscope, then cut into pieces (2–3 mm^3), and NP cells were released from the NP tissues by incubation with 0.25 mg/mL type II collagenase (Invitrogen, Carlsbad, CA) for 12 h at 37°C in Dulbecco's modified Eagle's medium (DMEM/F12; GIBCO, Grand Island, NY). After isolation, NP cells were resuspended in DMEM/F12 containing 10% fetal bovine serum (FBS; GIBCO), 100 mg/mL streptomycin, 100 U/mL penicillin, and 1% L-glutamine, and then incubated at 37°C in a humidified atmosphere with 5% CO_2. The confluent cells were detached by trypsinization and seeded into 35-mm tissue culture dishes in complete culture medium (DMEM/F12 supplemented with 10% FBS, 100 mg/mL streptomycin, and 100 U/mL penicillin) in a 37°C, 5% CO_2 environment. The medium was changed every 2 days. The third passage was used for subsequent experiments.

Quantitative real-time reverse transcription-polymerase chain reaction (qRT-PCR)

After RNA extraction, M-MLV reverse transcriptase (Invitrogen, Carlsbad, CA) was used to synthesize cDNA according to the manufacturer's instructions. The expression level of miR-3150a-3p was evaluated by qRT-PCR using a SYBR Green assay. PCR was performed in a 10-μL reaction volume, including 2 μL cDNA, 5 μL of 2× Master Mix, 0.5 μL forward primer (10 μM), 0.5 μL reverse primer (10 μM), and 2 μL double distilled water. The reaction was set at 95°C for 10 min for pre-denaturation, then at 95°C for 10 s and 60°C for 60 s repeating TargetScan cycles. Glyceraldehyde 3-phosphate dehydrogenase (GAPDH) was used as a reference. Both target and reference were amplified in triplicate wells. The relative level of each circular RNA was calculated using the $2^{-\Delta\Delta Ct}$ method [30]. The following primers were used: aggrecan (ACAN) forward: 5′-TGCATTCCACGAAGCTAACCTT-3′, reverse: 5′-GACGCCTCGCCTTCTTGAA-3′; GAPDH forward: 5′-AGAAAAACCTGCCAAATATGATGAC-3′, reverse: 5′-TGGGTGTCGCTGTTGAAGTC-3′; miR-3150a-3p forward: 5′-ACACTCCAGCTGGGCTGGGGAGATCCTCGA-3′, reverse: 5′-TGGTGTCGTGGAGTCG-3′; and U6 forward: 5′-CTCGCTTCGGCAGCACA-3′, reverse: 5′-AACGCTTCACGAATTTGCGT-3′.

Table 2. Dysregulated miRNAs in module "Blue"

miRNAs	logFC	adj.P Value
miR-3150a-3p	3.245100031	0.005804577
miR-4450	2.502310696	0.007702397
miR-887-3p	1.784873306	0.032300086
miR-4317	1.386439182	0.01254972
miR-516a-5p	1.296640795	0.049601398
miR-4758-5p	1.257113976	0.032300086
miR-3173-3p	-2.275445515	0.01254972
miR-299-5p	-2.318402227	0.005804577
miR-4657	-2.474131094	0.044148613
miR-4674	-2.522775577	0.011376461
miR-1273g-3p	-3.104570657	0.005804577
miR-1184	-4.75008002	0.005804577

Western blot analysis

Cultured cells were homogenized in lysis buffer (0.25 M Tris-HCl, pH 6.8, 20% glycerol, 4% sodium dodecyl sulfate [SDS], 10% mercaptoethanol) supplemented with protease and phosphatase inhibitors. Samples containing equal amounts of protein (10 μg) were electrophoresed on SDS-polyacrylamide gels. The proteins were then transferred to polyvinylidene fluoride membranes. Then, the membranes were blocked with 5% nonfat milk in Tris-buffered saline containing 0.1% Tween 20 (TBST) at room temperature for 1 h and incubated overnight at 4°C with primary antibodies diluted 1:3000 in TBST containing 5% nonfat milk. The secondary antibodies were used at a dilution of 1:6000 at room temperature for 1 h, and the immunoblots were developed by using an ECL system.

Cell transfection

NP cells from the third passage were used for transfection. Culture plates were incubated at 37°C in a humidified atmosphere with 5% CO_2. The cells were transfected with the corresponding plasmids or miRNA mimics using Lipofectamine 3000 (Invitrogen, Carlsbad, CA) according to the manufacturer's recommendations. The cells were harvested at 48 h after transfection.

Dual-luciferase reporter assay

ACAN was identified as a putative target gene of miR-3150a-3p. TargetScan and DIANA were used to predict target genes. The binding site in the 3′-untranslated region (UTR) of *ACAN*, called *ACAN*-wild-type (5′-GCCCAACCUUCUCCCCUCCCCAc-3′) and *ACAN*-mutant (5′-GCCCAACCUUCUCCCGAGGGGUc-3′), was inserted into the *Kpn*I and *Sac*I sites of the pGL3 promoter vector (Realgene, Nanjing, China) in a dual-luciferase reporter assay. Firstly, the cells were plated on 24-well plates. Then, 80 ng plasmid, 5 ng Renilla luciferase vector pRL-SV40, 50 nM miR-3150a-3p mimic (5′-GGUUGGAGCUCCUAGAGGGGUC-3′), and negative control were transfected into cells by using Lipofectamine 3000 (Invitrogen, Shanghai, China). The cells were collected and measured following the manufacturer's instructions by using a Dual-Luciferase Assay Kit (Promega, Madison, WI, USA) at 48 h after transfection. All experiments were repeated three times independently.

Statistical analysis

Each experiment was repeated at least three independent times, and the Schwann cells in each experiment were harvested from a single isolation. The results of qRT-PCR and the gray values from

western blot analysis are shown as the mean ± standard error of the mean(SEM). Statistical significance was determined using a two-tailed Student's t test (SPSS 22.0). The correlation between miR-3150a-3p expression and IDD grade, and the correlation between ACAN expression and IDD grade were analyzed using analysis of variance (ANOVA). The correlation of *ACAN* and miR-3150a-3p expression was assessed using Pearson's correlation analysis. Significance was set at *p < 0.05, **p < 0.01, or ***p < 0.001.

Results

Identification of IDD grade-associated co-expression miRNA network modules using WGCNA

After data normalization (Fig. 1), a total of 575 miRNAs were screened out from the expression profile of NP cells. WGCNA was performed with these 575 non-redundant miRNAs, leading to the identification of 16 WGCNA modules (Fig. 2A). Analysis of the module-trait relationships revealed that module "Blue" of 23 miRNAs was highly correlated with IDD grade (Pearson's correlation = 0.790, p = 0.007), while it was not correlated with age (Pearson's correlation = -0.1, p = 0.8) in the 10 samples (Fig. 2B). Therefore, the 23 miRNAs of module "Blue" were considered to have an important role in IDD.

Differentially expressed miRNAs of the WGCNA module highly associated with IDD grade

A total of 12 differentially expressed miRNAs were screened out from module "Blue," among which, 6 miRNAs were up-

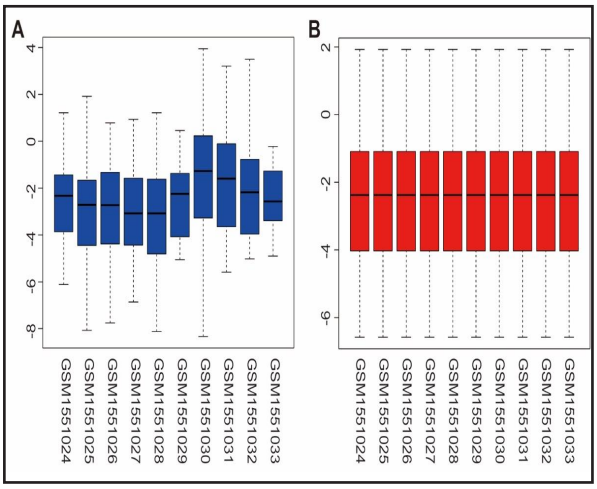

Fig. 1. Box plot for miRNA expression data. (A) miRNA data before normalization. (B) miRNA data after normalization. The medians (black lines) are almost at the same level, indicating the good performance of normalization.

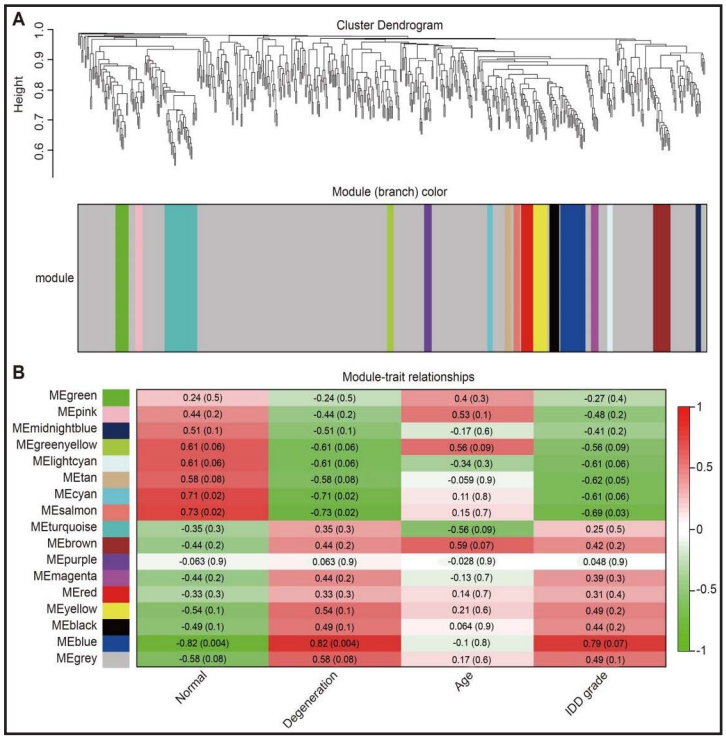

Fig. 2. WGCNA of miRNAs obtained from the Gene Expression Omnibus database. (A) Hierarchical cluster tree showing 16 modules of the co-expressed genes. Each of the 575 miRNAs is represented by a leaf in the tree, and each of the 16 modules by a major tree branch. The lower panel shows the modules in designated colors, such as "Blue," "Yellow," and "Turquoise." Note that module "Grey" is for unassigned miRNAs. (B) Module-trait correlations and corresponding p-values (in parentheses). The left panel shows the 16 modules. The color scale on the right shows module-trait correlation from -1 (green) to 1 (red).

regulated, while 6 miRNAs were down-regulated (Table 1). Hierarchical clustering showed that the miRNA expression pattern was distinguishable between IDD and normal control samples (Fig. 3). Notably, miR-3150a-3p was the most significantly up-regulated miRNA in module "Blue."

Validation of miR-3150a-3p expression by qRT-PCR

The miR-3150a-3p expression level was validated using qRT-PCR in 20 pairs of samples. As shown in Fig. 4A, miR-3150a-3p was significantly up-regulated in NP tissues from patients with IDD. In addition, when the IDD patients were grouped according to grade, miR-3150a-3p expression was significantly increased with the increase of grade (all $p < 0.05$) (Fig. 4A).

ACAN expression level and the correlation of miR-3150a-3p and ACAN

ACAN is the major non-collagenous component of the intervertebral disc. Degradation and loss of ACAN result in impairment of disc function and the onset of degeneration. In this study, as shown in Fig. 5A, the expression level of *ACAN* was significantly down-regulated in degenerative NP tissues. In addition, the expression level of *ACAN* was correlated with the expression level of miR-3150a-3p in NP tissues (Fig. 5B).

miR-3150a-3p downregulates ACAN expression

As predicted by TargetScan and DIANA, there

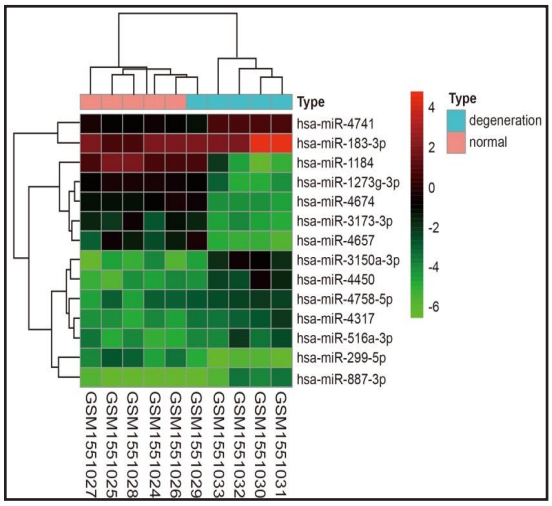

Fig. 3. Hierarchical cluster analysis of the significantly up- and down-regulated miRNAs in module "Blue." Each column represents a sample and each row represents an miRNA. A red strip represents high relative expression and a green strip represents low relative expression.

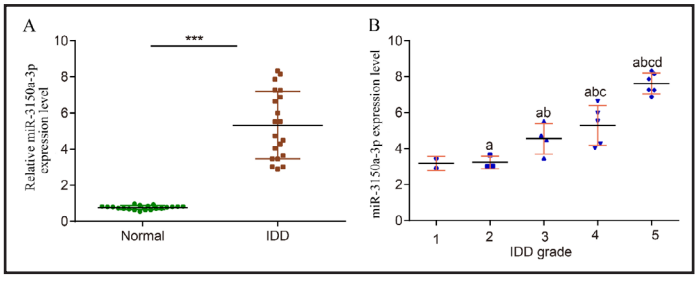

Fig. 4. Expression level of miR-3150a-3p in NP tissues in 20 patients and 20 controls using a qRT-PCR assay. (A) Expression of miR-3150a-3p in the normal and IDD groups. ***, $p<0.001$ compared with the normal group. (B) Expression of miR-3150a-3p in patients of different IDD grade. a, $p<0.05$ compared with grade 1; b, $p<0.05$ compared with grade 2; c, $p<0.05$ compared with grade 3; d, $p<0.05$ compared with grade 4.

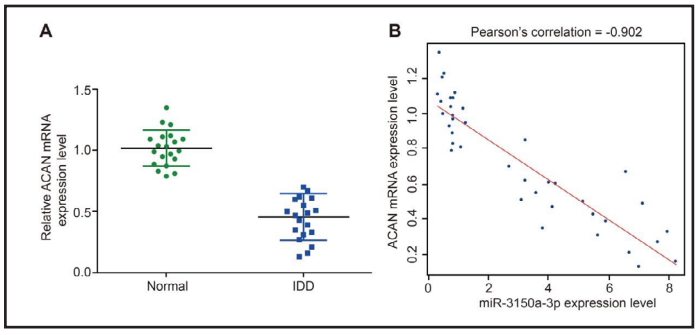

Fig. 5. Differential expression level of ACAN and the correlation of ACAN and miR-3150a-3p expression. (A) The expression level of ACAN was significantly down-regulated in degenerative NP tissues. ***, $p<0.001$. (B) The ACAN expression level was significantly negatively correlated with miR-3150a-3p expression (Pearson's correlation = -0.902, $p<0.0001$).

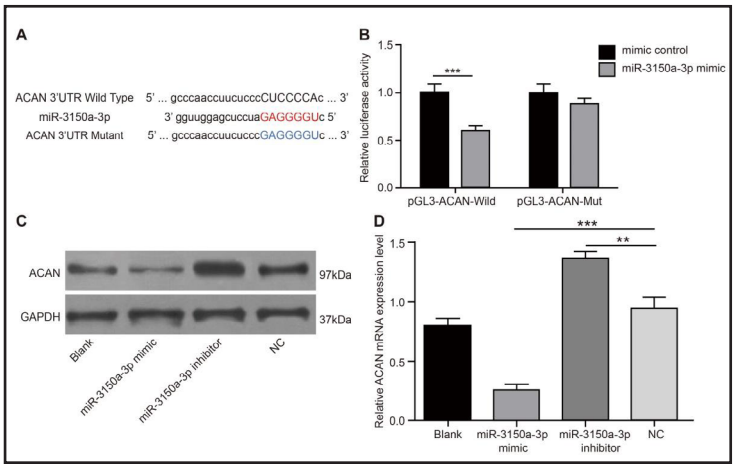

Fig. 6. Overexpression of miR-3150a-3p inhibits ACAN expression in NP cells. (A) Sequence alignment of human miR-3150a-3p with ACAN. Bottom: mutations in the ACAN sequence to create the mutant luciferase reporter construct. (B) Luciferase reporter assay in NP cells after transfection with negative control or miR-3150a-3p mimic, Renilla luciferase vector pRL-SV40, and the reporter construct. Both firefly and Renilla luciferase activities are measured in the same sample. Firefly luciferase signals were normalized with Renilla luciferase signals. (C–D) Overexpression of miR-3150a-3p decreased ACAN expression, whereas inhibition of miR-3150a-3p increased ACAN expression. Values are presented as the mean ± SEM. ***, p<0.001.

was complementarity between miR-3150a-3p and *ACAN*; the miR-3150a-3p sequence had a binding site for the 3′-UTR of wild-type *ACAN*, but without a binding site for the 3′-UTR of mutant *ACAN* (Fig. 6A). To confirm further the functional interaction between miR-3150a-3p and *ACAN* suggested by the target prediction algorithms, we performed luciferase reporter assays with an *ACAN* vector that contained either the putative 3′-UTR miR-3150a-3p binding site (wild-type) or mutant binding site (mutant). Overexpression of miR-3150a-3p significantly reduced the luciferase activity of the reporter gene for wild-type, but not mutant, indicating that miR-3150a-3p directly targeted the 3′-UTR of *ACAN* (Fig. 6B). This effect was further confirmed by protein and mRNA expression analyses. As shown in Fig. 6C–D, miR-3150a-3p overexpression decreased both *ACAN* protein and mRNA levels in NP cells, whereas inhibition of miR-3150a-3p increased *ACAN* levels. Taken together, these results demonstrated that miR-3150a-3p directly recognizes the 3′-UTR of *ACAN* mRNA and regulates its expression at the post-transcriptional level. More interestingly, when IDD patients were grouped according to different grades, ACAN expression was significantly increased with the increase of grade (all $p < 0.05$) (Fig. 7).

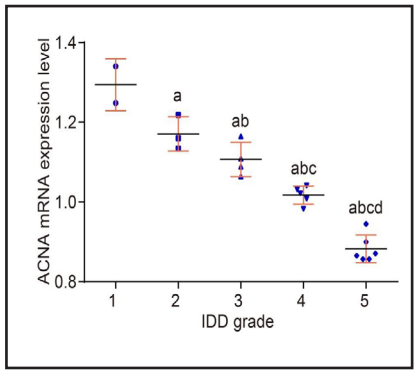

Fig. 7. Relationship between the expression of ACAN in IDD patients with different IDD grades by ANOVA. a, p<0.05 compared with grade 1; b, p<0.05 compared with grade 2; c, p<0.05 compared with grade 3; d, p<0.05 compared with grade 4.

Discussion

In the current study, we first performed WGCNA to identify IDD grade-related miRNAs, and module "Blue," which contains 23 miRNAs, was significantly correlated with IDD grade. Moreover, a total of 12 miRNAs was significantly dysregulated in module "Blue," and miR-3150a-3p was the most significantly up-regulated miRNA among these 12 miRNAs. Subsequently, we used qRT-PCR to confirm that miR-3150a-3p was significantly up-regulated in IDD patients compared with corresponding controls, and miR-3150a-3p

expression was significantly increased with the increase of IDD grade. The dysregulation of miR-3150a-3p has been observed in breast cancer. To date, the expression of miR-3150a-3p in degenerative NP tissues and its role in the development of IDD remain unclear. Thus, we selected miR-3150a-3p for further analysis. Current evidence suggests that loss of *ACAN* can be considered an early indicator of IDD. To investigate further the role of miR-3150a-3p in the pathogenesis of IDD, we performed functional analysis of miR-3150a-3p to investigate the relationship between miR-3150a-3p and *ACAN*. Notably, we identified *ACAN* to be a direct target gene of miR-3150a-3p, and *ACAN* expression was regulated by miR-3150a-3p. miR-3150a-3p overexpression decreased the expression of *ACAN* in NP cells, whereas inhibition of miR-3150a-3p increased the level of *ACAN*. In addition, *ACAN* expression was negatively correlated with IDD grade. These findings suggest that the reduction of *ACAN* expression induced by the upregulation of miR-3150a-3p might have a role in the development of IDD.

A hallmark of IDD is the progressive loss of extracellular matrix macro-molecules *ACAN* and collagen II [31]. *ACAN* abundance reaches a plateau in the early 20s, declining thereafter due to proteolysis, mainly by matrix metalloproteinases and aggrecanases, though the degradation of hyaluronan and non-enzymic glycation may also participate [32]. At present, there is no medical treatment for the repair of IDD, and ultimately surgical intervention is required for symptomatic relief. This can involve excision of a disc protrusion or, if degeneration is more extensive, removal of the whole disc followed by spinal fusion or the insertion of a disc prosthesis. These procedures are not ideal and do not restore normal disc function. In the case of fusion, the mechanics of the spine are altered and degeneration of the discs at levels adjacent to the fusion may result [33]. Thus, there is a need for a therapy that can retard or even halt the early degenerative process. As *ACAN* loss is a major driving force of early disc degeneration, it seems reasonable that such a therapy should ideally promote *ACAN* synthesis and at the same time prevent its degradation [34]. Single nucleotide variants of candidate genes in the *ACAN* metabolic pathway are associated with the severity of IDD and Modic changes in patients with chronic mechanical low back pain [35].

ACAN belongs to a family of proteoglycans that are characterized by the presence of glycosaminoglycan chains attached covalently to a core protein, and is the major non-collagenous component of the intervertebral disc. It is a large proteoglycan possessing numerous glycosaminoglycan chains and the ability to form aggregates in association with hyaluronan. Its abundance and unique molecular features provide the disc with its osmotic properties and ability to withstand compressive loads. In a healthy disc, swelling is mainly associated with the NP, where *ACAN* content is the highest, and is mainly resisted by the collagen fibrils of the surrounding annulus fibrosus. Upon applying compression to the tissue, water is displaced and the concentration of *ACAN* at the site of compression is increased, thereby increasing its swelling potential. This increased swelling potential is dissipated upon the removal of the compressive load as *ACAN* swells, drawing water back until the initial equilibrium is restored [32]. Degradation and loss of *ACAN* result in impairment of disc function and the onset of degeneration [36].

A previous study demonstrated that growth factors, such as bone morphogenetic protein 7, transforming growth factor β, and growth and differentiation factor 5, can repair a degenerative intervertebral disc in animal models by increasing *ACAN* content [37]. In this study, we demonstrated that miR-3150a-3p was significant up-regulated in degenerative NP cells (Fig. 4), whereas *ACAN* expression was negatively correlated with miR-3150a-3p expression (Fig. 5B). It is considered that the up-regulation of miR-3150a-3p expression inhibits *ACAN* in NP cells, thereby degrading extracellular matrix components, which might be the potential mechanism in human IDD.

Conclusion

This study provides the discovery and validation of IDD grade-associated miRNA expression profiles. We also demonstrated that miR-3150a-3p was significantly up-

regulated in human degenerative NP tissues, and that its level was associated with IDD grade. Importantly, miR-3150a-3p facilitates IDD by targeting *ACAN*. These findings should be valuable for a better understanding of the molecular mechanisms underlying the pathophysiology and molecular pathway of IDD, and should have important clinical significance in the prevention and treatment of degenerative discogenic diseases.

Acknowledgements

This study was supported by the State Key Program of the National Natural Science Foundation of China (81330042), the Special Program for Sino-Russian Joint Research Sponsored by the Ministry of Science and Technology, China (2014DFR31210), and the International Cooperation Program of the National Natural Science Foundation of China (81620108018).

Disclosure Statement

No conflict of interests exists.

References

1 Buckwalter JA: Aging and degeneration of the human intervertebral disc. Spine (Phila Pa 1976) 1995;20:1307-1314.
2 Costi JJ, Stokes IA, Gardner-Morse MG, Iatridis JC: Frequency-dependent behavior of the intervertebral disc in response to each of six degree of freedom dynamic loading: solid phase and fluid phase contributions. Spine (Phila Pa 1976) 2008;33:1731-1738.
3 Kalichman L, Hunter DJ: The genetics of intervertebral disc degeneration. Familial predisposition and heritability estimation. Joint Bone Spine 2008;75:383-387.
4 Samartzis D, Karppinen J, Mok F, Fong DY, Luk KD, Cheung KM: A population-based study of juvenile disc degeneration and its association with overweight and obesity, low back pain, and diminished functional status. J Bone Joint Surg Am 2011;93:662-670.
5 Friedman BW, O'Mahony S, Mulvey L, Davitt M, Choi H, Xia S, Esses D, Bijur PE, Gallagher EJ: One-week and 3-month outcomes after an emergency department visit for undifferentiated musculoskeletal low back pain. Ann Emerg Med 2012;59:128-133.e123.
6 Walker MH, Anderson DG: Molecular basis of intervertebral disc degeneration. Spine J 2004;4:158s-166s.
7 Ha KY, Koh IJ, Kirpalani PA, Kim YY, Cho YK, Khang GS, Han CW: The expression of hypoxia inducible factor-1alpha and apoptosis in herniated discs. Spine (Phila Pa 1976) 2006;31:1309-1313.
8 Ding F, Shao ZW, Xiong LM: Cell death in intervertebral disc degeneration. Apoptosis 2013;18:777-785.
9 Le Maitre CL, Freemont AJ, Hoyland JA: The role of interleukin-1 in the pathogenesis of human intervertebral disc degeneration. Arthritis Res Ther 2005;7:R732-745.
10 Zhao CQ, Liu D, Li H, Jiang LS, Dai LY: Interleukin-1beta enhances the effect of serum deprivation on rat annular cell apoptosis. Apoptosis 2007;12:2155-2161.
11 Zhao CQ, Jiang LS, Dai LY: Programmed cell death in intervertebral disc degeneration. Apoptosis 2006;11:2079-2088.
12 Matsui H, Kanamori M, Ishihara H, Yudoh K, Naruse Y, Tsuji H: Familial predisposition for lumbar degenerative disc disease. A case-control study. Spine (Phila Pa 1976) 1998;23:1029-1034.
13 Battie MC, Videman T, Kaprio J, Gibbons LE, Gill K, Manninen H, Saarela J, Peltonen L: The Twin Spine Study: contributions to a changing view of disc degeneration. Spine J 2009;9:47-59.
14 Bijkerk C, Houwing-Duistermaat JJ, Valkenburg HA, Meulenbelt I, Hofman A, Breedveld FC, Pols HA, van Duijn CM, Slagboom PE: Heritabilities of radiologic osteoarthritis in peripheral joints and of disc degeneration of the spine. Arthritis Rheum 1999;42:1729-1735.
15 Barrett T, Wilhite SE, Ledoux P, Evangelista C, Kim IF, Tomashevsky M, Marshall KA, Phillippy KH, Sherman PM, Holko M, Yefanov A, Lee H, Zhang N, Robertson CL, Serova N, Davis S, Soboleva A: NCBI GEO: archive for functional genomics data sets--update. Nucleic Acids Res 2013;41:D991-995.

16 Bentley DR, Balasubramanian S, Swerdlow HP, Smith GP, Milton J, Brown CG, Hall KP, Evers DJ, Barnes CL, Bignell HR, Boutell JM, Bryant J, Carter RJ, Keira Cheetham R, Cox AJ, Ellis DJ, Flatbush MR, Gormley NA, Humphray SJ, Irving LJ et al.: Accurate whole human genome sequencing using reversible terminator chemistry. Nature 2008;456:53-59.
17 Wheeler DA, Srinivasan M, Egholm M, Shen Y, Chen L, McGuire A, He W, Chen YJ, Makhijani V, Roth GT, Gomes X, Tartaro K, Niazi F, Turcotte CL, Irzyk GP, Lupski JR, Chinault C, Song XZ, Liu Y, Yuan Y, Nazareth L, Qin X, Muzny DM, Margulies M, Weinstock GM, Gibbs RA, Rothberg JM: The complete genome of an individual by massively parallel DNA sequencing. Nature 2008;452:872-876.
18 Brosnan CA, Voinnet O: The long and the short of noncoding RNAs. Curr Opin Cell Biol 2009;21:416-425.
19 Twayana S, Legnini I, Cesana M, Cacchiarelli D, Morlando M, Bozzoni I: Biogenesis and function of non-coding RNAs in muscle differentiation and in Duchenne muscular dystrophy. Biochem Soc Trans 2013;41:844-849.
20 Wang HQ, Yu XD, Liu ZH, Cheng X, Samartzis D, Jia LT, Wu SX, Huang J, Chen J, Luo ZJ: Deregulated miR-155 promotes Fas-mediated apoptosis in human intervertebral disc degeneration by targeting FADD and caspase-3. J Pathol 2011;225:232-242.
21 Liu G, Cao P, Chen H, Yuan W, Wang J, Tang X: MiR-27a regulates apoptosis in nucleus pulposus cells by targeting PI3K. PLoS One 2013;8:e75251.
22 Yu X, Li Z, Shen J, Wu WK, Liang J, Weng X, Qiu G: MicroRNA-10b promotes nucleus pulposus cell proliferation through RhoC-Akt pathway by targeting HOXD10 in intervetebral disc degeneration. PLoS One 2013;8:e83080.
23 Li Z, Yu X, Shen J, Chan MT, Wu WK: MicroRNA in intervertebral disc degeneration. Cell Prolif 2015;48:278-283.
24 Pfirrmann CW, Metzdorf A, Zanetti M, Hodler J, Boos N: Magnetic resonance classification of lumbar intervertebral disc degeneration. Spine (Phila Pa 1976) 2001;26:1873-1878.
25 Troyanskaya O, Cantor M, Sherlock G, Brown P, Hastie T, Tibshirani R, Botstein D, Altman RB: Missing value estimation methods for DNA microarrays. Bioinformatics 2001;17:520-525.
26 Fujita A, Sato JR, Rodrigues Lde O, Ferreira CE, Sogayar MC: Evaluating different methods of microarray data normalization. BMC Bioinformatics 2006;7:469.
27 Langfelder P, Horvath S: WGCNA: an R package for weighted correlation network analysis. BMC Bioinformatics 2008;9:559.
28 Law CW, Alhamdoosh M, Su S, Smyth GK, Ritchie ME: RNA-seq analysis is easy as 1-2-3 with limma, Glimma and edgeR. F1000Res 2016;5:1408.
29 Smyth GK: Linear models and empirical bayes methods for assessing differential expression in microarray experiments. Stat Appl Genet Mol Biol 2004;3:Article3.
30 Livak KJ, Schmittgen TD: Analysis of relative gene expression data using real-time quantitative PCR and the 2(-Delta Delta C(T)) Method. Methods 2001;25:402-408.
31 Matsui Y, Maeda M, Nakagami W, Iwata H: The involvement of matrix metalloproteinases and inflammation in lumbar disc herniation. Spine (Phila Pa 1976) 1998;23:863-868; discussion 868-869.
32 Sivan SS, Wachtel E, Roughley P: Structure, function, aging and turnover of aggrecan in the intervertebral disc. Biochim Biophys Acta 2014;1840:3181-3189.
33 Radcliff KE, Kepler CK, Jakoi A, Sidhu GS, Rihn J, Vaccaro AR, Albert TJ, Hilibrand AS: Adjacent segment disease in the lumbar spine following different treatment interventions. Spine J 2013;13:1339-1349.
34 Antoniou J, Steffen T, Nelson F, Winterbottom N, Hollander AP, Poole RA, Aebi M, Alini M: The human lumbar intervertebral disc: evidence for changes in the biosynthesis and denaturation of the extracellular matrix with growth, maturation, ageing, and degeneration. J Clin Invest 1996;98:996-1003.
35 Perera RS, Dissanayake PH, Senarath U, Wijayaratne LS, Karunanayake AL, Dissanayake VH: Single Nucleotide Variants of Candidate Genes in Aggrecan Metabolic Pathway Are Associated with Lumbar Disc Degeneration and Modic Changes. PLoS One 2017;12:e0169835.
36 Kepler CK, Ponnappan RK, Tannoury CA, Risbud MV, Anderson DG: The molecular basis of intervertebral disc degeneration. Spine J 2013;13:318-330.
37 Masuda K: Biological repair of the degenerated intervertebral disc by the injection of growth factors. Eur Spine J 2008;17 Suppl 4:441-451.